CONVOLUTIONAL NEURAL NETWORK (CNN) SUPPORTED URBAN DESIGN TO REDUCE PARTICLE AIR POLLUTANT CONCENTRATIONS

ZISHEN BAI[1] and CHENGZI PENG[2]
[1,2]*School of Architecture, The University of Sheffield.*
[1]*zbai5@sheffield.ac.uk, 0000-0002-8098-4729*
[2]*c.peng@sheffield.ac.uk, 0000-0001-8199-0955*

Abstract. PM2.5 has become a significant factor contributing to the haze outbreak in mainland China, which has negative impacts for public health. The current agility of CFD-based modelling to reveal in real-time the changes in PM2.5 concentrations in response to (proposed) changes in urban form limits its practical applications in the design processes. To support urban design for better air quality (AQ), this study presents a machine learning approach to test: (1) that the spatial distribution of PM2.5 concentrations measured in an urban area reflects the area's capacity to disperse particle air pollution; (2) that the PM2.5 concentration measurements can be linked to certain urban form attributes of that area. A Convolutional Neural Network algorithm called Residual Neural Network (ResNet) was trained and tested using the ChinaHighPM2.5 and urban form datasets. The result is a ResNet-AQ predictor for the city centre area in Beijing which had one of the highest air pollution levels within the Beijing-Tianjin-Hebei region. The urban area covered by the ResNet-AQ predictor contains 4,000 grid cells (approx. 25.3 km x 25.3 km), of which 1,200 (30%) cells were selected randomly for testing. The ResNet-AQ prediction accuracy achieved 87.3% after 100 iterations. An end-use scenario is presented to show how a social housing project can be supported by the AQ predictor to achieve better urban air quality performance.

Keywords. PM2.5, Urban Form Indicators, Image Classification, Convolutional Neural Network, Open Urban Data

1. Introduction

In recent years, the detrimental effects of air pollution on human health have attracted attention (Abdalla and Peng, 2021). China is ranked the most polluted country for air pollution among 175 countries globally (China MEE, 2020). PM2.5 consists of a high concentration of toxic and hazardous substances, which can be transported over long distances and have a long residence time in the atmosphere. PM2.5 significantly impacts atmospheric environmental quality and public health (Wang, 2017a).

Recent research on Urban Air Quality has focused on two areas. (1) Studies of

HUMAN-CENTRIC, Proceedings of the 28th International Conference of the Association for Computer-Aided Architectural Design Research in Asia (CAADRIA) 2022, Volume 1, 505-514. © 2023 and published by the Association for Computer-Aided Architectural Design Research in Asia (CAADRIA), Hong Kong.

traditional end-of-pipe treatments to reduce air pollutant emissions (Li and Zhou, 2019). A typical strategy was to reduce vehicle emissions by controlling urban road layouts (Rodríguez et al., 2016; Yuan et al., 2018). (2) Studies on reducing the pollutant stock in the air. A common approach was to improve air pollutant dispersion and deposition (Wang et al., 2017b). The effect of urban form on wind speed has been investigated via computational fluid dynamics (CFD), which further estimated the influence of wind speed on pollutant dispersion (Jia et al., 2021). Zhai et al. explored the effects of vegetation coverage on particle sedimentation based on computational fluid dynamics simulations (Zhai et al., 2022). Conventional CFD modelling requires detailed descriptions of the particle and fluid fields. CFD models may perform poorly due to inaccurate settings of urban form parameters and meteorological conditions (Jurado et al., 2021). Based on CFD outputs, a deep-learning neural network to predict air pollution was developed by Jurado et al. (2022) recognising that the CFD models were based on assumed parameters and could not fully reflect the real-world complexity. Due to the high computational cost, CFD remains problematic for architects and urban designers to evaluate urban air quality performance of design proposals in an interactive manner.

In this paper, we present a study of a modelling framework for urban air quality prediction to aid urban design based on satellite sensing data. In particular, near-surface PM2.5 concentrations derived from the Aerosol Optical Depth datasets have been made widely available by various agencies. Here, the main idea was to model the relationship between satellite imaging of PM2.5 concentrations and urban form characteristics at a city scale through Convolutional Neural Network (CNN) learning. A set of nine urban form indicators for characterising urban form was identified in our literature review, including Road Surface Density, Road Network Density, Natural Surface Ratio, Terrain Elevation, Building Density, Building Length, Building Volume, Average Building Height, and Building Height Difference. Both PM2.5 concentrations and urban form characteristics were pre-processed for CNN training and testing. Thus, urban design proposals drawn as master plans can be evaluated rapidly by the resultant CNN model to reveal the likely changes in urban air quality performance (i.e., PM2.5 concentrations) due to the proposed designs (changes).

2. Methods and materials

Figure 1 shows an overview of the workflow. The proposed modelling framework consists of three main parts: (1) Urban form data; (2) Urban PM2.5 concentration data; and (3) Training and testing Machine Learning algorithms. A major challenge was the acquisition and pre-processing of the urban form and urban air quality data required for the machine learning modelling. The quality (accuracy and resolution) of the datasets will determine the efficacy of the resultant model trained and tested as a location based urban air quality predictor, given the urban characteristics as inputs.

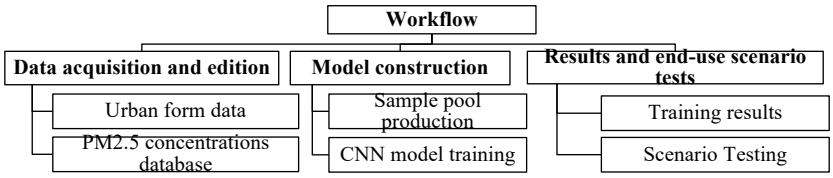

Figure 1. Workflow overview

2.1. URBAN FORM DATASET

A city map containing vector information is required to compute the nine urban form indicators. We used Open Street Map to obtain the urban form data in the ESRI Shapefile format (Marsudi, 2019). However, open street map does not provide valid building height information (Bernard et al., 2022). An alternative geo-data source, Amap (amap.com), one of the most popular web mapping service providers in China (Sun et al., 2020), provided building height data. A transformer application, Bigemap, was used in the study to acquire and transform the initial data from OSM. Furthermore, the NCDDC (National Coastal Data Development Center, https://www.ncddc.noaa.gov/) provides territorial elevation data, which can be input into ArcMap (version 10.8.1) directly as vector data.

Urban vector maps require the definition of the Geographic Coordinate System and Projected Coordinate System in ArcMap to make all processing work occur in the same coordinate system (Jekeli, 2006). In this study, the Chinese Geodetic Coordinate System 2000 was used, and the Gauss-Krüger projection method, currently expected in China, was used as the projected coordinate system (Yang, 2009).

The purpose of the urban form data editing is to generate a large set of training samples for image classification. Nine options of the grid resolution were examined for the study based on the fishnet function in ArcMap (Figure 2). While the low sample resolution (2 km x 2 km) can accommodate a wider urban area, the resultant sample size cannot be sufficient for machine learning. In contrast, the high-resolution sampling (50 m x 50 m) can produce the sample pool of a satisfactory size, but the small spatial coverage is inappropriate to the urban form indicators. Based on the assessment of the nine grid resolutions (Figure 2), the 400 m x 400 m resolution was chosen in this study to produce the final sample pool (N=4,000) for machine learning.

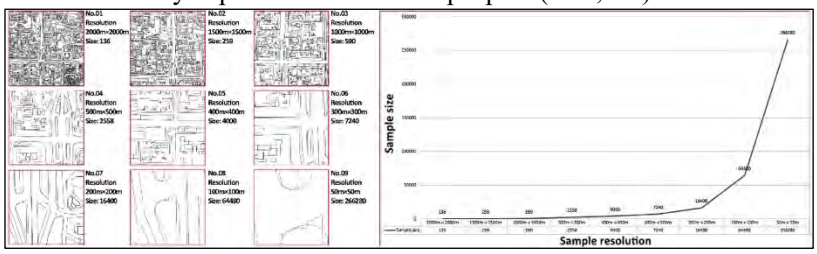

Figure 2. Urban grid size and resolution test

The next stage of the urban form data preparation involved colour labelling in

ArcMap, including the three vector layers labelled with different colours for defining urban form. Figure 3 shows the labelled sample images based on the Hexcone model in the RGB colour system. The red colour field shows the building height based on the three-metre gradient labels in the study area. Roads are in white colour, and natural surfaces are in green, reflecting the road surface density, road network density and natural surface density of the study area. Furthermore, the territorial height data provided by the NCDDC was labelled with a three-metre gradient of grey-scale shifts, which shows urban terrain changes in relative height.

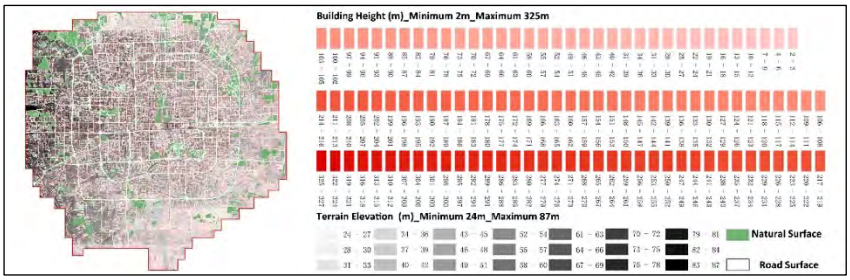

Figure 3. The urban form map of the study area tagged in ArcMap (v.10.8.1)

2.2. PM2.5 CONCENTRATION DATASET

Wei et al. (2021) employed the Moderate Resolution Imaging Spectroradiometer Multi-Angle implementation of Atmospheric Correction algorithm to estimate near-surface PM2.5 concentrations at a 1 km resolution. The output is the high resolution PM2.5 dataset for China (ChinaHighPM2.5), which was accessed for the Beijing central urban area in this study.

The image classification model (see Section 2.3) was trained on the urban form data samples (N=4,000), and each urban form sample (cell) was assigned a PM2.5 concentration value according to ChinaHighPM2.5. The assignment requires resampling where urban form grid cells crossing multiple PM2.5 concentration boundaries. Figure 4 shows the resampling method based on weighted average sum to ensure consistency in assigning PM2.5 concentrations to the urban from grid cells.

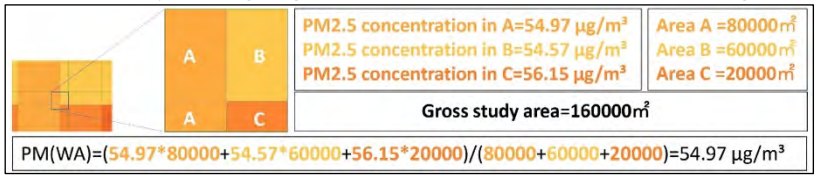

Figure 4. A weighted average algorithm for samples which cross concentration boundaries

The air quality monitoring network of the China Environmental Monitoring Center, CnOpenData, and Qingyue Open Data Center of Environment jointly provide the download service for accessing the ground based air quality monitoring data in China (He et al., 2021). There are 15 monitoring stations within the study area, providing monthly PM2.5 data for six years (2015-2020). The edited PM2.5 dataset prepared for the study area was then evaluated with three statistical measurements:

Determination (R^2), Root Mean Square Error (RMSE), and Mean Absolute Error (MAE). The sample size (N) is 90, and the statistical check gives R^2=0.96, RMSE=4.01 μg/m³ and MAE=2.98 μg/m³. The performance of the reassigned PM2.5 data is close to the source data provided by ChinaHighPM2.5 with R^2= 0.94, RMSE=5.07 μg/m³, and MAE=3.72 μg/m³ (Wei et al., 2021).

The training samples were further assessed the correlation of the PM2.5 with the urban form to identify the strongest correlation dataset. It is likely that the urban from samples and PM2.5 concentrations bear no correlation because of the instability of geospatial datasets and data latency (Zufle et al., 2020). A regression analysis was applied to determine the regression coefficient R^2 between urban form indicators and the annual mean PM2.5 concentration values from 2015 to 2020. Figure 5 shows the regression coefficients of PM2.5 concentrations and nine urban form indicators used in the study during the six-year period (2015-2020). The regression coefficient for the PM2.5 data in 2019 was the highest (R^2=0.30). As the study aims to achieve more sensitive classifiers in the image classification, the PM2.5 range is important, and the degree of fluctuations in the winter PM2.5 concentrations in 2019 shows a highest regression coefficient (R^2=0.37). Winter heating in northern China consume large quantities of fossil fuels and significantly increase PM2.5 concentrations (Liang et al., 2015). Thus, the winter months of January, February, November and December in 2019 were chosen for image classification training.

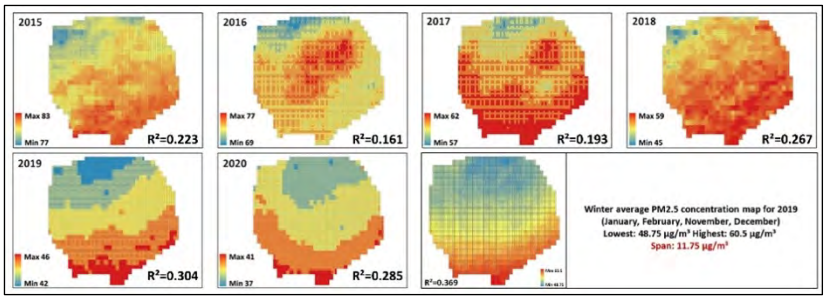

Figure 5. Regression coefficients of PM2.5 concentrations and urban form indicators in the study area for six years from 2015 to 2020

2.3. IMAGE CLASSIFICATION MODEL CONSTRUCTION

The study adopts a supervised classification learning approach to classify the input images (i.e., the urban form characterisation) using spectral features obtained from the training samples (Das, 2017). The urban form samples were applied for supervised classification training, and the category was based on the PM2.5 values of winter season 2019.

For efficient image printing of the samples, a simplified Python program was written (https://github.com/ZishenBai/GIS.git/). The program allows the printout to be saved based on a range of PM2.5 concentration levels. The advantage of the Python coding is efficient production and sample outputs and the program code is easily adjustable and reusable. The core import module for batch printing and classification saving is the Search-Cursor in ArcMap 10.8. 1. Search-Cursor is typically used to create read-only cursors on element classes or tables and allows the

use of where clause or field to restrict the query and sort results.

The image classification models were constructed and trained with the support of an online open resource no-code AI platform, EasyDL (https://ai.baidu.com/easydl/). EasyDL is an AI service development platform provided by Baidu Brain with deployable machine learning and deep learning algorithms (Singh, 2016). The main algorithm adopted for this study is the Deep Residual Learning algorithm, coded as ResNets on the EasyDL platform. ResNets has a strong track record, having won the best performance award at the ILSVRC 2015 computer vision competition (He et al., 2015). Due to the limitation of the sample pool size, an incremental training strategy was used in this study to improve the CNN model generalisation capability. In the urban form samples, a system of colour gradients was applied to different urban form indicators, meaning that warping or colour changes could potentially mislead the training models. An incremental training strategy with randomly occurring XY translation (TranslateX; TranslateY) with a 10% probability was selected for this study (Figure 6).

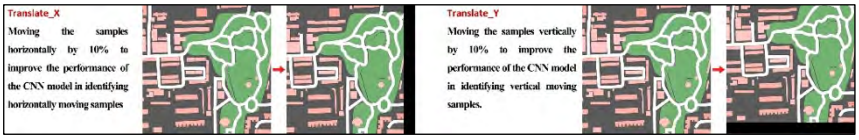

Figure 6. An incremental training strategy, based on a 10% XY translation

The final step was configuring the training environment based on the Baidu Public Cloud deployment service which provides the inference and prediction capabilities following the REST API style. The basic parameters of the model training server were Tesla P40, Video Mem: 24GB, CPU: 12 Cores, RAM: 40G.

3. Results and discussion

3.1. TRAINING RESULTS

In machine learning, image classification training generally involves optimising multiple training strategies, which can significantly affect the training results. In this study, all tests were based on the same training algorithm and test sample pool. The image classification model (function) was trained based on the supervised learning approach of the CNN framework using the ResNets algorithm. Table 1 shows the test results based on PM2.5 concentrations equally divided into five categories (levels), achieving an overall accuracy of 59.20%. The test report showed 93 samples confounded in Level_02 and Level_03, while only 7 were confounded in Level_02 and Level_05. This suggests that PM2.5 concentration levels cannot establish a significant relationship with the samples. Thus, the levels were reduced to four.

Table 1. Misclassification list for the test training

Label	Top 5 misidentified label size				Accuracy	Size
level_04	[79] level_05	[85] level_03	[46] level_02	[31] level_01	53.80%	260

level_02	[93] level_03	[78] level_01	[46] level_04	[07] level_05	52.50%	237
level_03	[93] level_02	[85] level_04	[35] level_01	[15] level_05	57.10%	264
level_01	[78] level_02	[35] level_03	[24] level_05	[31] level_04	66.70%	249
level_05	[79] level_04	[24] level_01	[15] level_03	[07] level_02	65.80%	185

Based on the test training results, the final model classification was defined as four categories according to four ranges of PM2.5 concentrations (Table 2). For each classification category (PM2.5 concentration level), 30% of the samples were randomly selected as the test set. After removing invalid samples, 3,800 samples (out of 4,000) were used, including 2,660 for training and 1,140 for testing. With 100 iterations of training (runtime: 5 hours and 16 minutes), the model achieved an accuracy of 87.30%.

Table 2. Classification results checklist

Category	Level_01	Level_02	Level_03	Level_04
PM2.5 concentrations	48.75μg/m³-52.00μg/m³	52.01μg/m³-54.00μg/m³	54.01μg/m³-57.00μg/m³	57.01μg/m³-60.50μg/m³

3.2. AN END-USE SCENARIO

To illustrate how the Beijing ResNets-AQ Predictor as trained may be applied in urban design practice, the Baiziwan social housing project, located on the fourth ring road in the Beijing city centre (39.89 ° N, 116.51 ° E), was evaluated as an end-use test scenario. The affordable housing project was completed by MAD Studio in 2021 (Iype, 2021). The ResNets-AQ Predictor was applied to compare the PM2.5 concentration levels of the urban area before and after the Baiziwan social housing project. Figure 7 shows the outcome of the testing. It shows that the PM2.5 concentration of the site before the social housing project was estimated at Level_03 (probability of 56.06%) and Level_04 (41.07%), indicating the winter PM2.5 concentrations would be in the range of 54.01μg/m³ - 60.50μg/m³ (probability of 97.13%). The PM2.5 concentration levels after the Baiziwan Social Housing Project was estimated at Level_02 (64.38%) and Level_03 (30.90%), indicating the winter PM2.5 concentrations would be in the range of 52.01μg/m³ - 57.00μg/m³ (probability of 95.28%). The PM2.5 concentration values and predicted probabilities for the top two levels of the test results were used to assess the effect of the social housing project in terms of PM2.5 concentrations through a weighted average estimation. The results show that the PM2.5 concentration at the site was 55.24 μg/m³ (before) and 51.27 μg/m³ (after), indicating that the social housing project leads to about 7.19% reduction in PM2.5 concentrations. As such, this end-use test scenario shows an example of how the ResNets-AQ Predictor can be applied to generate rapid air quality assessments of urban design proposals without going through site-specific CFD modelling and simulation. The runtime invested in the ResNets-AQ predictor training and testing delivers the agility required of interactive design processes.

Figure 7. Assessment results (a) Site before regeneration, (b) Baiziwan social housing project

The numerical predictions can be complemented by adding links to related air quality literature to further improve the usability of the ResNets-AQ Predictor for rapid evaluation of existing urban areas as well as proposed interventions. For this test use scenario, firstly, the social housing project has significantly reduced the building density on the site, decreasing wind obstruction (Yang et al., 2020). The new buildings were designed with reduced windward sides and increased distances between buildings, which potentially increased the wind speed within the site and accelerated PM2.5 dispersion rates (Yang et al., 2020). Furthermore, the project has significantly increased natural surface areas, raising the sedimentation impact of vegetation on PM2.5 (Wang et al., 2014; Cheng et al., 2015). Vertical landscaping can reduce dust pollution due to increased wind speeds by high-rise buildings. However, the project has increased road density, potentially increasing PM2.5 concentrations. There is a synergistic effect between the road surface density and road network density indicators, and generally, a wider road network with lower density has the potential to decrease PM 2.5 concentrations (Wang et al., 2017b). In conclusion, the renewed urban form with reduced PM2.5 concentrations is primarily attributable to the change in wind speed and the increase in vegetation area. Thus, the ResNets-AQ predictive evaluation was considered to be in an agreement with an observation of the urban form features introduced by the Baiziwan social housing project.

4. Conclusion and further work

The study presents an urban air quality modelling tool built on the CNN-based image classification technique. The main purpose of the tool is to enable rapid assessment of urban form performance in terms of PM2.5 concentrations during high ambient air pollution months. A contribution of the study is the development of a novel modelling framework that creates links between satellite aerosol sensing data and urban form characterisation at an urban scale. Unlike the conventional CFD approach, the data-driven deep learning method can provide the agility required in rapid interaction with design decision-making. It can be anticipated that designers will be able to interact with a ResNets-AQ evaluation/prediction platform via mobile devices and receive likely PM2.5 concentration levels of their design proposals.

Following this study, there are a number of areas to be further investigated. Firstly, a ResNets-AQ predictor is location based, that is, the Beijing ResNets-AQ predictor can only be applied to urban areas/projects in Beijing. However, the modelling methods and techniques are expected to be applicable to other cities.

Further work on other cities' datasets will provide such a verification. Secondly, the non-linear relationship between PM2.5 concentrations and urban form, and the autocorrelation among some indicators (Haining, 2003), should be considered in further development. Thirdly, further integration with Multi-Objective Optimisation could extend the utility of an urban air quality platform by providing not only assessment but also recommended steps or moves to achieve improvements.

Researchers have recently proposed training pix2pix models with a Generative Adversarial Network to build generative machine learning frameworks (Yao et al., 2021). A future multi-objective optimisation framework realisation could make a breakthrough by moving into the emerging field of interaction design with AI, or machine learning assisted design.

References

Abdalla, T. E., & Peng, C. (2021). Evaluation of housing stock indoor air quality models: A review of data requirements and model performance. *Journal of Building Engineering*, 43, 102846. https://doi.org/10.1016/j.jobe.2021.102846

Bernard, J., Bocher, E., Le Saux Wiederhold, E., Leconte, F., & Masson, V. (2022). Estimation of missing building height in OpenStreetMap data: a French case study using GeoClimate 0.0. 1. *Geoscientific Model Development Discussions*, 1-47. https://doi.org/10.5194/gmd-15-7505-2022

Ministry of Ecology. (2022). *2020 Press Conference Records of Ministry of Ecology and Environment, the People's Republic of China. Springer Nature*. Taken from: http://www.mee.gov.cn/hjzl/sthjzk/zghjzkgb/

Rodríguez, M. C., Dupont-Courtade, L., & Oueslati, W. (2016). Air pollution and urban structure linkages: Evidence from European cities. *Renewable and Sustainable Energy Reviews*, 53, 1-9. https://doi.org/10.1016/j.rser.2015.07.190

Cheng, Y., He, K. B., Du, Z. Y., Zheng, M., Duan, F. K., & Ma, Y. L. (2015). Humidity plays an important role in the PM2. 5 pollutions in Beijing. *Environmental pollution*, 197, 68-75. https://doi.org/10.1016/j.envpol.2014.11.028

Das, T. (2017). *Machine Learning algorithms for Image Classification of hand digits and face recognition dataset. Machine Learning*, 4(12), 640-649.

Haining, R. P., & Haining, R. (2003). *Spatial data analysis: theory and practice*. Cambridge university press. http://dx.doi.org/10.1017/CBO9780511754944

He, K., Zhang, X., Ren, S., & Sun, J. (2015). *Deep residual learning for image recognition*. cite. arXiv preprint arxiv:1512.03385. https://doi.org/10.1109/CVPR.2016.90

He, Q., Gao, K., Zhang, L., Song, Y., & Zhang, M. (2021). Satellite-derived 1-km estimates and long-term trends of PM2. 5 concentrations in China from 2000 to 2018. *Environment international*, 156, 106726. https://doi.org/10.1016/j.envint.2021.106726

Iype, J (2021) *MAD's first social housing project Baiziwan integrates community into urban fabric*. Available at: https://www.stirworld.com/see-features-mad-s-first-social-housing-project-baiziwan-integrates-community-into-urban-fabric/ (Accessed: 17 August 2022).

Jekeli, C. (2006). Geometric reference systems in geodesy. Division of Geodesy and Geospatial Science, *School of Earth Sciences*, Ohio State University, 25.

Jia, B., Liu, S., & Ng, M. (2021). *Air quality and key variables in high-density housing. Sustainability*, 13(8), 4281. https://doi.org/10.3390/su13084281

Jurado, X., Reiminger, N., Vazquez, J., & Wemmert, C. (2021). On the minimal wind directions required to assess mean annual air pollution concentration based on CFD results. *Sustainable Cities and Society*, 71, 102920. doi.org/10.1016/j.scs.2021.102920

Jurado, X., Reiminger, N., Benmoussa, M., Vazquez, J., & Wemmert, C. (2022). Deep learning methods evaluation to predict air quality based on Computational Fluid

Dynamics. *Expert Systems with Applications*, 203, 117294. https://doi.org/10.1016/j.eswa.2022.117294

Liang, X., Zou, T., Guo, B., Li, S., Zhang, H., Zhang, S., Huang, H., & Chen, S. X. (2015). Assessing Beijing's PM 2.5 pollution: severity, weather impact, APEC and winter heating. Proceedings of the Royal Society. A, *Mathematical, Physical, and Engineering Sciences*, 471(2182), 20150257. https://doi.org/10.1098/rspa.2015.0257

Li, F., & Zhou, T. (2019). Effects of urban form on air quality in China: An analysis based on the spatial autoregressive model. *Cities*, 89, 130-140. https://doi.org/10.1016/j.cities.2019.01.025

Marsudi, I. (2019). *Extraction of Open Street Map to Produce Digital Maps. In IOP Conference Series: Earth and Environmental Science.* Vol. 366, No. 1, p. 012025. IOP Publishing. https://doi.org/10.1088/1755-1315/366/1/012025

Singh, J. (2016). *Baidu unveils open-source deep learning platform PaddlePaddle*.=

Sun, J., Wang, H., Song, Z., Lu, J., Meng, P., & Qin, S. (2020). Mapping essential urban land use categories in nanjing by integrating multi-source big data. *Remote Sensing*, 12(15), 2386. https://doi.org/10.3390/RS12152386

Wang, Q., Sandberg, M., Lin, Y., Yin, S., & Hang, J. (2017). Impacts of urban layouts and open space on urban ventilation evaluated by concentration decay method. *Atmosphere*, 8(9), 169. https://doi.org/10.3390/atmos8090169

Wang, S., Zhou, C., Wang, Z., Feng, K., & Hubacek, K. (2017). The characteristics and drivers of fine particulate matter (PM2. 5) distribution in China. *Journal of Cleaner Production*, 142, 1800-1809. https://doi.org/10.1016/j.jclepro.2016.11.104

Wang, X., Liu, C., Kostyniuk, L., Shen, Q., & Bao, S. (2014). The influence of street environments on fuel efficiency: insights from naturalistic driving. *International Journal of Environmental Science and Technology*, 11(8), 2291-2306. https://doi.org/10.1007/s13762-014-0584-1

Wei, J., Li, Z., Lyapustin, A., Sun, L., Peng, Y., Xue, W., Su, T., and Cribb, M. (2021). Reconstructing 1-km-resolution high-quality PM2.5 data records from 2000 to 2018 in China: spatiotemporal variations and policy implications, Remote Sensing of Environment (252), 112136, doi.org/10.1016/j.rse.2020.112136.

Yao, J., Huang, C., Peng, X. I., & Yuan, P. F. (2021). *Generative design method of building group-Based on generative adversarial network and genetic algorithm*. Proceedings of the 26th International Conference of the Association for Computer-Aided Architectural Design Research in Asia (CAADRIA) 2021, Volume 1, 61-70.

Yang, Y. (2009). *Chinese geodetic coordinate system 2000*. Chinese Science Bulletin, 54(15), 2714-2721. https://doi.org/10.1007/s11434-009-0342-9

Yuan, M., Song, Y., Huang, Y., Hong, S., & Huang, L. (2018). Exploring the association between urban form and air quality in China. *Journal of Planning Education and Research*, 38(4), 413-426. https://doi.org/10.1177/0739456X17711516

Yang, J., Shi, B., Zheng, Y., Shi, Y., & Xia, G. (2020). Urban form and air pollution disperse: Key indexes and mitigation strategies. *Sustainable Cities and Society*, 57, 101955. https://doi.org/10.1016/j.scs.2019.101955

Zhai, H., Yao, J., Wang, G., & Tang, X. (2022). Impact of Land Use on Atmospheric Particulate Matter Concentrations: A Case Study of the Beijing–Tianjin–Hebei Region, China. *Atmosphere*, 13(3), 391. https://doi.org/10.3390/atmos13030391

Züfle, A., Trajcevski, G., Pfoser, D., & Kim, J. S. (2020, June). *Managing uncertainty in evolving geo-spatial data. In 2020 21st IEEE International Conference on Mobile Data Management (MDM) (pp. 5-8)*. IEEE. https://doi.org/10.1109/MDM48529.2020.00021